

Thermal energy reactions of $\text{CO}^+ 2$ with chloromethanes

Masaharu Tsuji, Tsuyoshi Funatsu, Kenichi Matsumura, and Yukio Nishimura

Citation: *The Journal of Chemical Physics* **99**, 4526 (1993); doi: 10.1063/1.466052

View online: <http://dx.doi.org/10.1063/1.466052>

View Table of Contents: <http://scitation.aip.org/content/aip/journal/jcp/99/6?ver=pdfcov>

Published by the [AIP Publishing](#)

Articles you may be interested in

[Thermal energy charge-transfer reactions: \$\text{He}^+ 2\$ with \$\text{N}_2\$ and \$\text{CO}\$](#)

J. Chem. Phys. **79**, 5368 (1983); 10.1063/1.445700

[Thermal Energy Reactions of \$\text{C}^-\$ with \$\text{O}_2\$, \$\text{N}_2\text{O}\$, \$\text{CO}\$, and \$\text{CO}_2\$](#)

J. Chem. Phys. **53**, 2614 (1970); 10.1063/1.1674379

[Rate Constants for the Thermal Energy Reactions of \$\text{H}^-\$ with \$\text{O}_2\$, \$\text{NO}\$, \$\text{CO}\$, and \$\text{N}_2\text{O}\$](#)

J. Chem. Phys. **53**, 987 (1970); 10.1063/1.1674168

[Erratum: "Thermal Energy Ion—Neutral Reaction Rates. IV. Nitrogen Ion Charge Transfer Reactions with \$\text{CO}\$ and \$\text{CO}_2\$ "](#)

J. Chem. Phys. **46**, 2019 (1967); 10.1063/1.1840991

[Thermal Energy Ion—Neutral Reaction Rates. IV. Nitrogen Ion Charge Transfer Reactions with \$\text{CO}\$ and \$\text{CO}_2\$](#)

J. Chem. Phys. **44**, 4537 (1966); 10.1063/1.1726670



Thermal energy reactions of CO_2^+ with chloromethanes

Masaharu Tsuji, Tsuyoshi Funatsu,^{a)} Ken-ichi Matsumura, and Yukio Nishimura
Institute of Advanced Material Study and Department of Molecular Science and Technology, Graduate School of Engineering Sciences, Kyushu University, Kasuga-shi, Fukuoka 816, Japan

(Received 13 April 1993; accepted 2 June 1993)

Rate constants and product ions have been determined for thermal energy reactions of CO_2^+ with $\text{CH}_n\text{Cl}_{4-n}$ ($n=0-3$) by using an ion-beam apparatus. Total rate constants are (8.7 ± 3.7) , (6.7 ± 3.1) , (9.1 ± 4.1) , and $(4.9 \pm 1.6) \times 10^{-10} \text{ cm}^3 \text{ s}^{-1}$ for CH_3Cl , CH_2Cl_2 , CHCl_3 , and CCl_4 , respectively. These values amount to 38%–61% of the collision rate constants estimated from either the Langevin or averaged dipole oriented theory. Although charge transfer followed by the successive loss of a Cl atom is the major product channel, parent ions are formed from CH_3Cl and CH_2Cl_2 with branching ratios of $33\% \pm 5\%$ and $25\% \pm 3\%$, respectively. The reaction mechanisms are interpreted in terms of the electronic states of the parent molecular ion accessible in the charge-transfer processes. The lack of formation of parent ions from CHCl_3 and CCl_4 is explained as due to complete (pre)dissociation of ionic states below 13.78 eV.

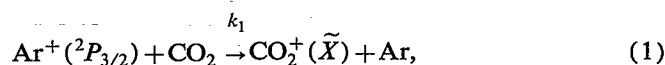
I. INTRODUCTION

We have recently studied charge-transfer (CT) reactions of Ar^+ with $\text{CH}_n\text{Cl}_{4-n}$ ($n=0-3$) at thermal energy by using an ion-beam apparatus.^{1,2} The product ion distributions and rate constants were determined. Near-resonant CT followed by the successive loss of a H or Cl atom was the major product channel observed. The smaller rate constant for CCl_4 compared with those of $\text{CH}_n\text{Cl}_{4-n}$ ($n=1-3$) were qualitatively explained by the lack of an energy-resonant ionic state with favorable Franck-Condon factors (FCFs) for vertical ionization. However, the relation $k_{\text{obs}} \geq 0.42 k_{\text{calc}}$ [Langevin or averaged dipole oriented (ADO) theory] holds for all the reactions, indicating that the existence of favorable FCFs is not a significant factor for assessing the magnitude of the rates of $\text{Ar}^+/\text{CH}_n\text{Cl}_{4-n}$ CT reactions.

Compared with extensive studies on thermal energy CT reactions of rare gas ions, little work has been carried out on those of molecular ions. Since the discovery of a large amount of the CO_2^+ ion in the Martian and Venus atmospheres,^{3,4} there has been continuous interest in ion-molecule reactions of CO_2^+ with simple molecules.^{5,6} To the best of our knowledge, there has been only one report on thermal CT reactions of CO_2^+ with halogenated methanes by Copp *et al.*⁶ They have determined the rate constant and product ion distribution for the $\text{CO}_2^+/\text{CH}_3\text{Cl}$ reaction at 298 K by using a selected ion flow tube (SIFT) method. Here, we study thermal CT reactions of CO_2^+ with $\text{CH}_n\text{Cl}_{4-n}$ ($n=0-3$) by using the low-energy ion-beam apparatus. An advantage of our beam apparatus is that the operating pressure is much lower than that used in the SIFT method, so that secondary collisions by the buffer gas are reduced greatly. The rate constants and product ion distributions are determined and compared with the previous SIFT data. The dissociation processes are discussed by reference to reported photoelectron spectroscopic data of parent cations.

II. EXPERIMENT

The thermal ion-beam apparatus used in the present study was similar to that used for the $\text{Ar}^+/\text{CH}_n\text{Cl}_{4-n}$ reaction^{1,2} except for the addition of a CO_2 inlet in a reactant ion source. In brief, a mixture of the ground-state $\text{Ar}^+(^2P_{3/2,1/2})$ ions, high energy metastable ($\text{Ar}^+)^*$ ions, and the metastable $\text{Ar}(^3P_{0,2})$ atoms were generated by a microwave discharge of high purity Ar gas in a quartz flow tube.⁷ The metastable ($\text{Ar}^+)^*$ ions were more rapidly quenched than $\text{Ar}^+(^2P_{3/2,1/2})$ while flowing in a quartz tube. Therefore, a long distance of about 30–40 cm between the microwave discharge and the CO_2 gas inlet was used to isolate $\text{Ar}^+(^2P_{3/2,1/2})$. There are two spin-orbit states, $\text{Ar}^+(^2P_{3/2})$ and $\text{Ar}^+(^2P_{1/2})$, with recombination energies of 15.76 and 15.92 eV, respectively. The lack of the upper $\text{Ar}^+(^2P_{1/2})$ component and the presence of the lower $\text{Ar}^+(^2P_{3/2})$ component in the Ar flowing afterglow were confirmed by observing $\text{ArF}(B-X, D-X)$ excimers resulting from the spin-orbit state selective $\text{Ar}^+(^2P_{1/2,3/2}) + \text{SF}_6^-$ ionic-recombination reaction.^{8,9} The metastable $\text{Ar}(^3P_{0,2})$ atoms were completely quenched by the addition of CO_2 . The $\text{CO}_2^+(\tilde{X})$ ions were produced by the thermal energy CT reaction of Ar^+ with CO_2 :



$$k_1 = (5.6 \pm 1.3) \times 10^{-10} \text{ cm}^3 \text{ s}^{-1} \text{ (Refs. 10 and 11).}$$

After being completely thermalized by collisions with the buffer Ar gas, CO_2^+ ions were expanded into a low-pressure chamber through a molybdenum nozzle (2 mm in diameter) centered on the flow tube. The vibrational frequency of the ν_1 mode in $\text{CO}_2^+(\tilde{X})$ is 1280 cm^{-1} ,¹² and hence less than 0.2% of $\text{CO}_2^+(\tilde{X})$ would be populated in the vibrational excited state at 300 K. Therefore, it is expected that the contribution of vibrationally excited $\text{CO}_2^+(\tilde{X})$ was insignificant under the present experimental condition.

The sample gas was kept at a constant mass flow and injected from a stainless steel orifice placed 5 cm downstream from the nozzle. The reactant and product ions

^{a)}Present address: NEC Corporation, Tamagawa, Nakahara-ku, Kawasaki, 211.

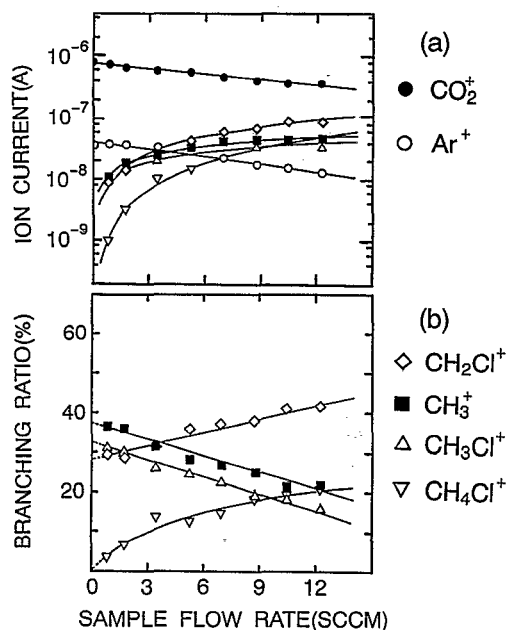


FIG. 1. The variation of (a) the reactant and product ion currents and (b) the percentages of the ionic products with CH_3Cl flow for the $\text{CO}_2^+/\text{CH}_3\text{Cl}$ reaction. As a reference, the decay of Ar^+ with the addition of CH_3Cl under the same experimental conditions is shown in (a).

were sampled through a molybdenum orifice (2 mm in diameter), placed 3 cm further downstream, and analyzed using an ULVAC MSQ 400 quadrupole mass spectrometer. The mass spectra were averaged using a Kenwood DCS-8200 digital storage oscilloscope and stored in a microcomputer. Operating pressures were (0.5–0.7) Torr (1 Torr = 133.3 Pa) in the flowing afterglow ion-source chamber, $(2.0\text{--}3.5) \times 10^{-3}$ Torr in the reaction chamber, and $(0.8\text{--}2.0) \times 10^{-5}$ Torr in the mass analyzing chamber.

III. RESULTS AND DISCUSSION

A. Rate constants

Figures 1(a), 2(a), 3, and 4 show semilogarithmic plots of CO_2^+ and product ion currents vs a reagent flow rate for the $\text{CO}_2^+/\text{CH}_n\text{Cl}_{4-n}$ ($n=0\text{--}3$) reactions. Total rate constants $k_{\text{CO}_2^+}$ are determined from the decay of CO_2^+ , which is governed by the pseudo-first-order rate law,

$$I(\text{CO}_2^+) = I_0(\text{CO}_2^+) \exp(-k_{\text{CO}_2^+} [\text{CH}_n\text{Cl}_{4-n}] t). \quad (2)$$

Here, $[\text{CH}_n\text{Cl}_{4-n}]$ is the sample gas concentration and t is the reaction time. The t value is given by $t = L/\langle v \rangle$, where L is the reaction path length from the sample gas inlet to the sampling orifice and $\langle v \rangle$ is an average relative velocity. Since it was difficult to evaluate the accurate t value, the $k_{\text{CO}_2^+}$ values were evaluated with reference to the previously measured rate constants of the $\text{Ar}^+/\text{CH}_n\text{Cl}_{4-n}$ reactions (k_{Ar^+}).^{1,2} Assuming a beam-gas cell condition, the $\langle v \rangle$ value is proportional to $(M)^{-1/2}$ based upon gas kinetic theory, where M is the mass of a reactant ion. Thus, the following relation was used for the estimation of the $k_{\text{CO}_2^+}$ values.

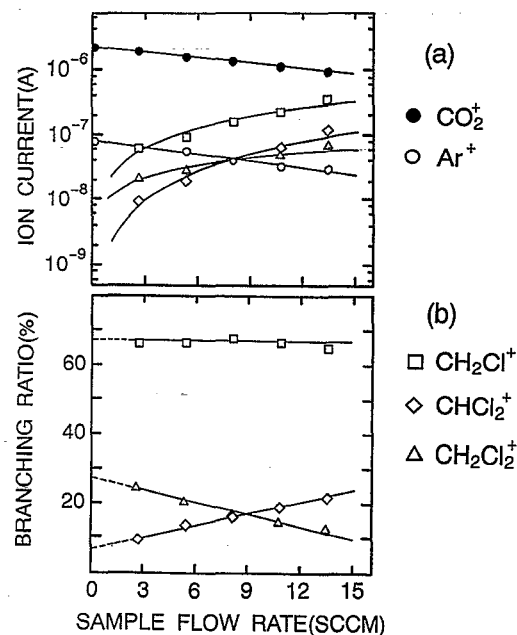


FIG. 2. The variation of (a) the reactant and product ion currents and (b) the percentages of the ionic products with CH_2Cl_2 flow for the $\text{CO}_2^+/\text{CH}_2\text{Cl}_2$ reaction. As a reference, the decay of Ar^+ with the addition of CH_2Cl_2 under the same experimental conditions is shown in (a).

$$k_{\text{CO}_2^+} = k_{\text{Ar}^+} \frac{\ln \{I(\text{CO}_2^+)/I_0(\text{CO}_2^+)\} (M_{\text{Ar}^+})^{1/2}}{\ln \{I(\text{Ar}^+)/I_0(\text{Ar}^+)\} (M_{\text{CO}_2^+})^{1/2}}. \quad (3)$$

The decay of Ar^+ with the addition of $\text{CH}_n\text{Cl}_{4-n}$ under the same experimental conditions are shown in Figs. 1(a), 2(a), 3, and 4. The observed rate constants obtained from slopes of linear semilogarithmic plots are summarized in Table I. The accuracies of the present data for $k_{\text{CO}_2^+}$ are estimated by summing up an experimental error of $k_{\text{CO}_2^+}$ and uncertainties of the reported k_{Ar^+} values. In Table I are also given the calculated collision rate constants from the Langevin¹⁵ or ADO¹⁶ theory, the energy difference between the recombination energy of CO_2^+ and the adiabatic

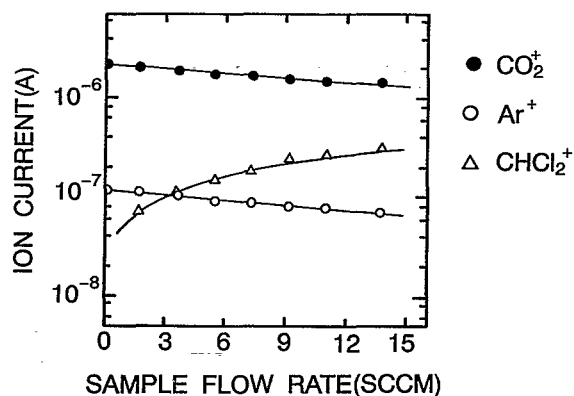


FIG. 3. The variation of the reactant and product ion currents with CHCl_3 flow for the $\text{CO}_2^+/\text{CHCl}_3$ reaction. As a reference, the decay of Ar^+ with the addition of CHCl_3 under the same experimental conditions is shown.

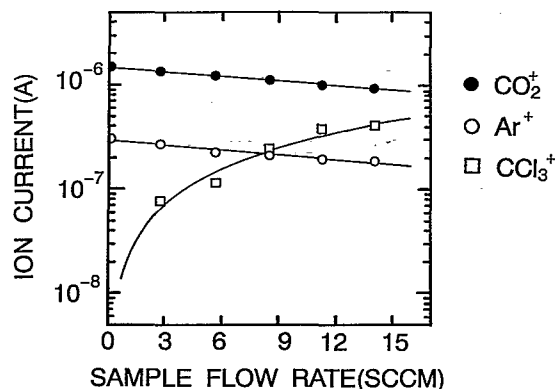


FIG. 4. The variation of the reactant and product ion currents with CCl_4 flow for the $\text{CO}_2^+/\text{CCl}_4$ reaction. As a reference, the decay of Ar^+ with the addition of CCl_4 under the same experimental conditions is shown.

ionization potential (IP_a) of $\text{CH}_n\text{Cl}_{4-n}$ (ΔE), and the dipole moments and polarizabilities (α) of $\text{CH}_n\text{Cl}_{4-n}$ ($n=0-3$). The most obvious feature of the data is the complete absence of a dependence of the rate constant on the ionic ground-state exothermicity of the reaction. A similar independence of the reactivity on the exothermicity has been obtained in the CT reactions between Ar^+ and $\text{CH}_n\text{Cl}_{4-n}$ ($n=0-4$).^{1,2} According to an ion-cyclotron-resonance (ICR) study by Laudenslager *et al.*,^{17,18} the thermal CT reactions of rare gas ions with simple molecules are fast when there is an energy resonant state with favorable FCFs for ionization. On the other hand, valid information about the importance of FCFs could not be obtained for the reactions of molecular O_2^+ , N_2^+ , and CO^+ , and CO_2^+ with CH_4 in an ICR study of Ausloos *et al.*¹⁹ In order to determine the relative importance of the FCFs in the present systems, the reported photoelectron spectra (PES) of $\text{CH}_n\text{Cl}_{4-n}$ are compared with the recombination energy of the reactant CO_2^+ ion in Fig. 5. Energy resonant states with favorable FCFs are absent in all cases. However, it should be noted that the CT reactions are fast ($k_{\text{obs}}/k_{\text{calc}} \geq 0.38$). It may therefore be reasonable to assume that the existence of favorable FCFs is not the appropriate criterion for assessing the magnitude of the rates of $\text{CO}_2^+/\text{CH}_n\text{Cl}_{4-n}$ CT reactions at thermal energy.

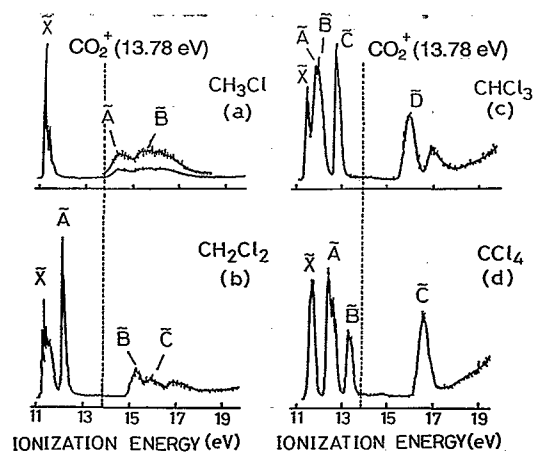


FIG. 5. Photoelectron spectra of $\text{CH}_n\text{Cl}_{4-n}$ ($n=0-3$). The broken lines indicate the recombination energy of CO_2^+ . Adopted from Ref. 20.

B. Product ion distribution

1. $\text{CO}_2^+ + \text{CH}_3\text{Cl}$

In addition to the CH_3Cl^+ , CH_2Cl^+ , and CH_3^+ ions, the secondary CH_4Cl^+ ion was detected in the $\text{CO}_2^+/\text{CH}_3\text{Cl}$ reaction. From the raw data shown in Fig. 1(a), the dependence of branching ratios of each product ion on the CH_3Cl flow rate is obtained, as shown in Fig. 1(b). By decreasing the CH_3Cl flow rate, the branching ratios of CH_3Cl^+ and CH_3^+ increase, while those of CH_2Cl^+ and CH_4Cl^+ decrease and approach 28% and zero at zero CH_3Cl flow rate, respectively. On the basis of these facts and known reactions of the CH_3Cl system,^{10,21-24} it is concluded that CH_3Cl^+ , CH_2Cl^+ , and CH_3^+ are produced from primary $\text{CO}_2^+/\text{CH}_3\text{Cl}$ reaction (4), whereas a part of CH_2Cl^+ and all of CH_4Cl^+ are produced from secondary reactions (5) and (6), respectively,

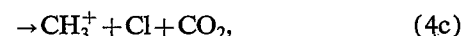
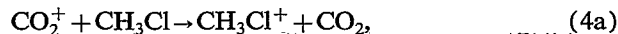


TABLE I. Observed and calculated reaction rate constants, reaction exothermicity, and dipole moments and polarizabilities of $\text{CH}_n\text{Cl}_{4-n}$.

Reactions	k_{obs}^b ($10^{-10} \text{ cm}^3 \text{ s}^{-1}$)	k_{calc}^a ($10^{-10} \text{ cm}^3 \text{ s}^{-1}$)	$k_{\text{obs}}/k_{\text{calc}}$	ΔE^b (eV)	Dipole moment ^c (D)	α^c (\AA^3)
$\text{CO}_2^+ + \text{CH}_3\text{Cl}$	8.7 ± 3.7	18	0.48 ± 0.21	2.52	1.87	5.35
$\text{CO}_2^+ + \text{CH}_2\text{Cl}_2$	6.7 ± 3.1	16	0.42 ± 0.19	2.43	1.60	6.48
$\text{CO}_2^+ + \text{CHCl}_3$	9.1 ± 4.1	15	0.61 ± 0.27	2.36	1.01	9.5
$\text{CO}_2^+ + \text{CCl}_4$	4.9 ± 1.6	13	0.38 ± 0.12	2.31	0.00	10.5

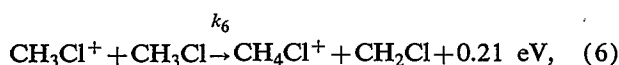
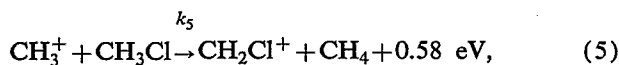
^aCalculated from Langevin or ADO theory.

^b $\text{RE}(\text{CO}_2^+) - \text{IP}_a(\text{CH}_n\text{Cl}_{4-n}(\bar{X}))$.

^cReferences 13 and 14.

TABLE II. Product ion distributions in the CO₂⁺/CH_nCl_{4-n} (n=0-3) charge-transfer reactions at thermal energy.

Reactant molecule	Product ion	Appearance potential (eV) ^a	Branching ratio (%)	
			This work	Copp <i>et al.</i> ^b
CH ₃ Cl	CH ₃ Cl ⁺	11.26	33±5	60±10
	CH ₂ Cl ⁺	12.98	28±5	40±10
	CH ₃ ⁺	13.87	39±5	
CH ₂ Cl ₂	CH ₂ Cl ₂ ⁺	11.33	25±3	
	CHCl ₂ ⁺	12.12	8±3	
	CH ₂ Cl ⁺	12.89	67±3	
CHCl ₃	CHCl ₃ ⁺	11.42		
	CHCl ₂ ⁺	11.6	100	
	CCl ₂ ⁺	12.2		
CCl ₄	CCl ₄ ⁺	11.47		
	CCl ₃ ⁺	11.67	100	

^aReference 25.^bReference 6.

where the ΔH° values are calculated from reported thermochemical data.²⁵ The k_5 value has been estimated to be $9.7 \times 10^{-10} \text{ cm}^3 \text{ s}^{-1}$ by employing high-pressure mass spectroscopy at a reactant ion energy of 0.21 eV,²¹ though the product ion has not been identified. The k_6 value at thermal energy has been measured as 2.65 and $1.70 \times 10^{-9} \text{ cm}^3 \text{ s}^{-1}$ by using a high-pressure mass spectrometer.^{22,23}

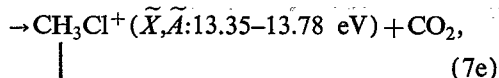
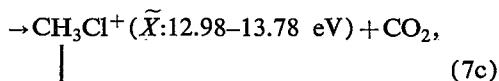
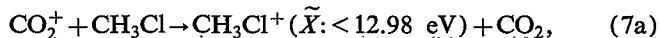
By extrapolating the percentages of each product ion to zero CH₃Cl flow, the initial branching ratios of each product ion are determined. The results obtained are given in Table II along with the previous SIFT data of Copp *et al.*⁶ It should be noted that our beam data is significantly different from their SIFT data in which no CH₃⁺ has been detected. A similar difference has recently been found in the product ion distribution of the Ar⁺/CH₄ reaction between our beam experiment (CH₃⁺:CH₂⁺ = 85% ± 1%:15% ± 1%)²⁶ and the SIFT experiment of Shul *et al.*, (CH₄⁺:CH₃⁺:CH₂⁺ = 10% ± 2%:79% ± 4%:11% ± 2%).^{11,27} Since the CH₂⁺/CH₄ and CH₃⁺/CH₄ ion-molecule reactions do not give CH₄⁺,¹⁰ these reactions can be excluded from possible secondary reactions leading to CH₄⁺ in their SIFT experiment. According to the photoelectron-photoion coincidence (PEPICO) data for CH₄⁺,²⁸ the parent CH₄⁺ ion arises from the CH₄⁺(\bar{X}) state in the 12.7–14.5 eV region, while the CH₃⁺ and CH₂⁺ ions are produced from higher states above 14.30 and 15.18 eV, respectively. On the basis of these facts, the discrepancy between the beam and SIFT data on the Ar⁺/CH₄ reaction has been attributed to collisional relaxation of the CH₄⁺* precursor state in the energy range 14.6–15.76 eV by the buffer gas in the SIFT experiment which operates at much higher pressures. As described below, the CH₃⁺ ion is formed through dissociation of the \bar{X} and/or \bar{A} state in the 13.35–13.78 eV region, while the CH₃Cl⁺ ion arises from

low vibrational levels of the \bar{X} state below 12.98 eV. Therefore, the lack of CH₃⁺ and the high branching ratio of CH₃Cl⁺ in the SIFT data of Copp *et al.*⁶ may also be due to collisional relaxation of the precursor CH₃Cl⁺(\bar{A}, \bar{X}) states to the lower CH₃Cl⁺(\bar{X}) state. According to our optical spectroscopic studies on Penning ionization and CT reactions,^{29–32} the vibrational and rotational relaxation and the electronic quenching by collisions with a buffer gas have been found for molecular ions with radiative lifetimes longer than ~500 ns in the flowing afterglow [e.g., HCl⁺(\bar{A}), O₂⁺(\bar{A}), H₂O⁺(\bar{A}), and CS₂⁺(\bar{A})]. Thus, the lifetimes of the precursor CH₃Cl⁺(\bar{A}, \bar{X}) states may be longer than ~500 ns.

Figure 5(a) shows PES of CH₃Cl in the 13–18 eV range, where the \bar{X}^2E , \bar{A}^2A_1 , and \bar{B}^2E states with vertical ionization potentials (IP_v) of 11.29, 14.42, and 15.47 eV, respectively, are present. On the basis of *ab initio* calculations of molecular orbitals (MO),²⁰ MO's characters of removed electron have been estimated to be n_{Cl} for the \bar{X} state, σ_{Cl} for the \bar{A} state, and π_{CH_3} (pseudo) for the \bar{B} state. According to the PEPICO data of Eland *et al.*,³³ the ground \bar{X} state, which correlates to the CH₂Cl⁺+H and CH₃⁺+Cl dissociation limits at 12.98 and 13.35 eV,^{25,33} respectively, is bound. Therefore, the parent cation is produced from the low vibrationally excited \bar{X} state in the 11–12 eV region. The \bar{A} state fully dissociates into CH₃⁺+Cl. Eighty percent of the \bar{B} state decays by the $\bar{B} \rightarrow \bar{A}$ internal conversion and the rest dissociates into CH₂Cl⁺+H.

On the basis of the PEPICO data, the parent CH₃Cl⁺ ion is dominantly produced via low vibrational levels of the \bar{X} state below the lowest dissociation limit of 12.98 eV, whereas the CH₃⁺ ion is formed through dissociation of the \bar{X} and/or \bar{A} state in the 13.35–13.78 eV region. The appearance potential of CH₃⁺ from CH₃Cl has been measured to be 13.87 eV in photoionization.³⁴ The detection of CH₃⁺ in the thermal CO₂⁺/CH₃Cl reaction suggests that its appearance potential in the ion-molecule reaction must be lower than the recombination energy of CO₂⁺ (13.78 eV). The higher appearance potential in the photoionization is probably due to the low probability of photoionization into lower dissociation levels with poor vertical FCFs. Although the appearance potential of CH₂Cl⁺ has been measured as 12.98 eV, no PEPICO signal has been obtained near this energy. Eland *et al.*³³ concluded that the higher vibrational levels of the \bar{X} state, whose energy is sufficient for H loss, are not populated in vertical photoionization of CH₃Cl. It should be noted that a significant amount of CH₂Cl⁺ (28% ± 5%) is formed in the CO₂⁺/CH₃Cl reaction. Since the recombination energy of CO₂⁺ is 13.78 eV, the formation of CH₂Cl⁺ from the \bar{B} state is energetically inaccessible in the CO₂⁺/CH₃Cl reaction. It is therefore likely that the CH₂Cl⁺ ion arises from dissociation of the near-resonant high vibrationally excited \bar{X} state above 12.98 eV for which FCFs for vertical ionization is negligibly small. The large k_{obs} value for the CO₂⁺/CH₃Cl reaction can be explained by populating vibrational states having poor Franck-Condon overlap. Summing up the above

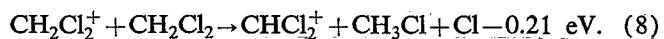
results, the dominant reaction scheme of the $\text{CO}_2^+/\text{CH}_3\text{Cl}$ system is represented by



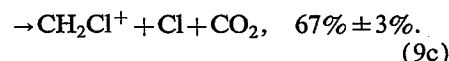
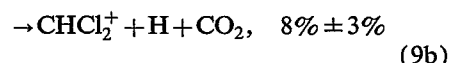
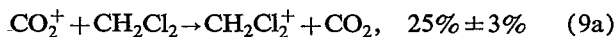
Since the CH_2Cl^+ and CH_3^+ ions are formed through CH_3Cl^+ states above 12.98 eV, 67% of the total reaction occurs as near-resonant CT within 0.80 eV. On the other hand, more than 0.80 eV is imparted as relative translational energy of products and/or internal energy of CO_2 for the formation of the parent ion. Such a nonresonant reaction occupies 33% of the total product channel. We have recently found that CT reactions of Ar^+ with simple aliphatic hydrocarbons such as CH_4 , C_2H_4 , and C_2H_6 occur near resonantly without a significant momentum transfer and that about 88%–95% of the excess energy is converted into internal energy of the product ions.²⁶ Although the parent C_2H_4^+ ion is produced through nonresonant CT in the $\text{Ar}^+/\text{C}_2\text{H}_4$ reaction, its branching ratio is only $4\% \pm 1\%$. The relatively high branching fraction of CH_3Cl^+ in the $\text{CO}_2^+/\text{CH}_3\text{Cl}$ reaction implies that the fraction of nonresonant CT is larger than that in the Ar^+ reactions. The degrees of freedom in the products, which can accept the excess energy, increases in the CO_2^+ reactions in comparison with those in the Ar^+ reactions. Therefore, the probability of the nonresonant CT becomes large.

2. $\text{CO}_2^+ + \text{CH}_2\text{Cl}_2$

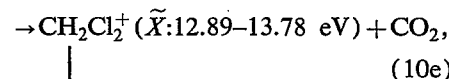
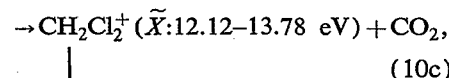
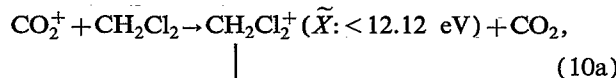
The $\text{CO}_2^+/\text{CH}_2\text{Cl}_2$ reaction yields CH_2Cl_2^+ , CH_2Cl^+ , and CHCl_2^+ , as shown in Fig. 2(a). In Fig. 2(b) the dependence of the branching ratios of each product ion on the CH_2Cl_2 flow rate is presented. The branching ratio of CH_2Cl^+ is independent of the CH_2Cl_2 flow rate. With increasing CH_2Cl_2 flow rate, the branching ratio of CHCl_2^+ increases, whereas that of CH_2Cl_2^+ decreases. This indicates that the following secondary reaction participates in the formation of CHCl_2^+ ,



The CH_2Cl_2^+ ion produced in the present experiment is expected to maintain some internal and kinetic energies because of low operating pressures. Thus, the formation of CHCl_2^+ through endoergic process (8) becomes energetically accessible. The initial product ion distribution is obtained from the data shown in Fig. 2(b):

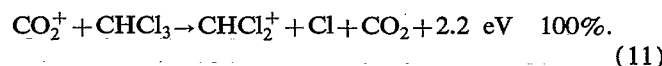


Energetically possible precursor CH_2Cl_2^+ states are \tilde{X} ($\text{IP}_v = 11.40 \text{ eV}$) and \tilde{A} (12.22 eV) arising from loss of an electron with n_{Cl} character [see PES in Fig. 5(b)].²⁰ The MO's character of the ejected electrons is consistent with the experimental observation that the major product arises from loss of a Cl atom. The appearance potentials of CHCl_2^+ and CH_2Cl^+ are 12.12 and 12.89 eV, respectively. By analogy with the dissociation pattern of CH_3Cl^+ , it is highly likely that the CHCl_2^+ ion results from (pre)dissociation of vibrationally excited levels of the \tilde{X} state above 12.12 eV, while the major CH_2Cl^+ ion is produced from the \tilde{A} state in the 12.89–13.78 eV region. It should be noted that the parent CH_2Cl_2^+ ion is formed with a relatively high branching ratio of $25\% \pm 3\%$. It is dominantly produced through low vibrationally excited levels of the \tilde{X} state below 12.12 eV in which at least 1.66 eV must be released as relative translational energy and internal energies of CH_2Cl_2^+ and CO_2 . The detection of CH_2Cl_2^+ implies that such nonresonant CT leading to low energy \tilde{X} state takes place, though its branching ratio is smaller than that of near-resonant CT leading to the CH_2Cl^+ fragment. Summing up the above results, the fragmentation pattern of CH_2Cl_2^+ in the $\text{CO}_2^+/\text{CH}_2\text{Cl}_2$ reaction is given by:



3. $\text{CO}_2^+ + \text{CHCl}_3$

Figure 3 shows that the $\text{CO}_2^+/\text{CHCl}_3$ reaction yields exclusively the CHCl_2^+ fragment with an appearance potential of 11.6 eV,

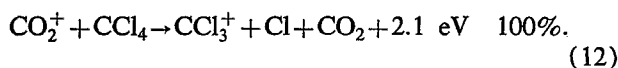


In the $\text{CO}_2^+/\text{CH}_4$ reaction, not only CT leading to the parent CH_4^+ ion, but also hydrogen atom transfer leading to CO_2H^+ occurs with a high branching ratio of about 72%.^{10,35} However, such a hydrogen atom transfer channel is closed in the reactions of CO_2^+ with chlorinated methanes based on the present data.

Possible precursor CHCl_3^+ states for the formation of CHCl_2^+ are \bar{X} ($\text{IP}_v = 11.48$ eV), \bar{A} (11.91 eV), \bar{B} (12.01 eV), and \bar{C} (12.85 eV) [see PES in Fig. 5(c)].²⁰ All of these states arise from the loss of an electron with n_{Cl} character, which is in agreement with the experimental observation. The CHCl_2^+ ion must result from (pre)dissociation of these ionic states in the 11.6–13.78 eV region. Since the energy of the \bar{C} state is closer to the recombination energy of CO_2^+ than the energies of the \bar{X} , \bar{A} , and \bar{B} states, the \bar{C} state would be the most important precursor state for the CHCl_2^+ production. It should be noted that the parent CHCl_3^+ ion cannot be detected in the $\text{CO}_2^+/\text{CHCl}_3$ reaction, though the IP_v value of the ionic ground state is comparable with those of CH_3Cl and CH_2Cl_2 . CHCl_3^+ has not been detected in electron-impact ionization³⁶ and Penning ionization by the $\text{He}(2^3S)$ and $\text{Ne}(3P_{0,2})$ atoms.³⁷ The appearance potential of CHCl_2^+ , 11.6 eV, is close to an adiabatic ionization potential of the \bar{X} state, 11.42 eV.²⁵ On the basis of these findings, the dominant reason for the lack of the parent ion is attributed to the fact that CHCl_3^+ is fully dissociative in the 11.42–13.78 eV region. Although the formation of CCl_2^+ with an appearance potential of 12.2 eV is energetically allowed, it was not detected. This suggests that elimination channel of HCl from CHCl_3^+ is closed in the $\text{CO}_2^+/\text{CHCl}_3$ reaction.

4. $\text{CO}_2^+ + \text{CCl}_4$

The $\text{CO}_2^+/\text{CCl}_4$ reaction provides only CCl_3^+ , as shown in Fig. 4.



Possible precursor CCl_4^+ states are \bar{X}^2T_1 ($\text{IP}_v = 11.69$ eV), \bar{A}^2T_2 (12.62 eV), and/or \bar{B}^2E (13.44 eV) with a n_{Cl} character [see PES in Fig. 5(d)].²⁰ According to the PEPICO data,³⁸ all of these states fully dissociate into $\text{CCl}_3^+ + \text{Cl}$, which is in agreement with the MO's character. Therefore, the lack of CCl_4^+ can be explained as due to the absence of stable CCl_4^{+*} states below 13.78 eV. Among these possible precursor states, the highest \bar{B} state is probably most important for the formation of CCl_3^+ because the major product channels in the $\text{CO}_2^+/\text{CH}_3\text{Cl}$ and $\text{CO}_2^+/\text{CH}_2\text{Cl}_2$ reactions are near-resonant CT.

C. Summary

Thermal energy reactions of CO_2^+ with $\text{CH}_n\text{Cl}_{4-n}$ ($n = 0-3$) have been investigated by using an ion-beam apparatus. The rate constants and product distributions were determined and summarized in Tables I and II, respectively. Total rate constants amount to 38%–61% of the collision rate constants estimated from either the Langevin or ADO theory, though FCFs for ionization are small. Therefore, it was concluded that FCFs are not important in governing the reaction rate in the present reaction system. For all reactions, only CT product channels were observed and no evidence of hydrogen atom transfer channels was found. The product ion distributions led us to conclude that nonresonant CT, as well as near-resonant CT occurs in the $\text{CO}_2^+/\text{CH}_n\text{Cl}_{4-n}$ ($n = 0-3$) reactions. The

occurrence of nonresonant CT was explained as due to a large number of degrees of freedom in the product channels.

ACKNOWLEDGMENTS

This work was supported by a Grant-in-Aid for Scientific Research from the Japanese Ministry of Education, Science, and Culture (Grant No. 02555170), the Asahi Glass Foundation, the Ito Science Foundation, and the Morino Foundation for molecular science.

- ¹M. Tsuji, M. Funatsu, H. Kouno, and Y. Nishimura, *Chem. Phys. Lett.* **192**, 362 (1992).
- ²M. Tsuji, T. Funatsu, H. Kouno, Y. Nishimura, and H. Obase, *J. Chem. Phys.* **97**, 8216 (1992).
- ³M. B. McElroy, *J. Geophys. Res.* **73**, 1513 (1968).
- ⁴A. I. Stewart, *J. Geophys. Res.* **77**, 54 (1972).
- ⁵A. B. Rakshit and P. Warneck, *J. Chem. Soc. Faraday Trans. 2*, **76**, 1084 (1980).
- ⁶N. W. Copp, M. Hamdan, J. D. C. Jones, K. Birkinshaw, and N. D. Twiddy, *Chem. Phys. Lett.* **88**, 508 (1982).
- ⁷M. Tsuji, in *Techniques of Chemistry*, edited by J. M. Farrar and W. H. Saunders, Jr. (Wiley, New York, 1988), Vol. 20, Chap. 9, p. 489.
- ⁸M. Tsuji, M. Furusawa, and Y. Nishimura, *J. Chem. Phys.* **92**, 6502 (1990).
- ⁹M. Tsuji, M. Ide, T. Muraoka, and Y. Nishimura, *J. Chem. Phys.* (in press).
- ¹⁰Y. Ikezoe, S. Matsuoka, M. Takebe, and A. Viggiano, *Gas-Phase Ion-Molecule Reaction Rate Constants Through 1986* (Maruzen, Tokyo, 1987), and references therein.
- ¹¹R. J. Shul, B. L. Upschulte, R. Passarella, R. G. Keesee, and A. W. Castleman, Jr., *J. Phys. Chem.* **91**, 2556 (1987).
- ¹²G. Herzberg, *Electronic Spectra and Electronic Structure of Polyatomic Molecules* (Van Nostrand Reinhold, New York, 1966).
- ¹³*CRC Handbook of Chemistry and Physics*, edited by R. C. Weast, M. J. Astle, and W. H. Beyer, 68th ed. (CRC, Boca Raton, FL, 1988).
- ¹⁴*Kagaku Benran*, Vol. II, edited by the Japanese Chemical Society (Maruzen, Tokyo, 1984), p. 320 (in Japanese).
- ¹⁵G. Gioumoussis and D. P. Stevenson, *J. Chem. Phys.* **29**, 294 (1958).
- ¹⁶T. Su, E. C. F. Su, and M. T. Bowers, *J. Chem. Phys.* **69**, 2243 (1978).
- ¹⁷J. B. Laudenslager, W. T. Huntress, Jr., and M. T. Bowers, *J. Chem. Phys.* **61**, 4600 (1974).
- ¹⁸V. G. Anicich, J. B. Laudenslager, W. T. Huntress, Jr., and J. H. Futrell, *J. Chem. Phys.* **67**, 4340 (1977).
- ¹⁹P. Ausloos, J. R. Eyler, and S. G. Lias, *Chem. Phys. Lett.* **30**, 21 (1975).
- ²⁰K. Kimura, S. Katsumata, Y. Achiba, T. Yamazaki, and S. Iwata, *Handbook of HeI Photoelectron Spectra of Fundamental Organic Molecules* (Japan Science Society, Tokyo, 1981).
- ²¹A. A. Herod, A. G. Harrison, and N. A. McAskill, *Can. J. Chem.* **49**, 2217 (1971).
- ²²A. G. Harrison and J. C. J. Thynne, *Trans. Faraday Soc.* **64**, 1287 (1968).
- ²³S. K. Gupta, E. G. Jones, A. G. Harisson, and J. J. Myher, *Can. J. Chem.* **45**, 3107 (1967).
- ²⁴J. L. Beauchamp, D. Holtz, S. D. Woodgate, and S. L. Patt, *J. Am. Chem. Soc.* **94**, 2798 (1972).
- ²⁵H. M. Rosenstock, K. Draxl, B. W. Steiner, and J. T. Herron, *J. Phys. Chem. Ref. Data* **6**, Suppl. 1 (1977).
- ²⁶M. Tsuji, H. Kouno, K. Matsumura, T. Funatsu, Y. Nishimura, H. Obase, H. Kugishima, and K. Yoshida, *J. Chem. Phys.* **98**, 2011 (1993).
- ²⁷R. Shul, R. Passarella, X. L. Yang, R. G. Keesee, and A. W. Castleman, Jr., *J. Chem. Phys.* **87**, 1630 (1987).
- ²⁸R. Stockbauer, *J. Chem. Phys.* **58**, 3800 (1973).
- ²⁹M. Tsuji, J. P. Maier, H. Obase, and Y. Nishimura, *Chem. Phys.* **110**, 17 (1986).
- ³⁰M. Tsuji and J. P. Maier, *Chem. Phys.* **126**, 425 (1988).

- ³¹M. Tsuji, J. P. Maier, H. Obase, and Y. Nishimura, *Chem. Phys. Lett.* **147**, 619 (1988).
- ³²M. Tsuji, H. Obase, M. Endoh, S. Yamaguchi, K. Yamaguchi, K. Koburai, and Y. Nishimura, *J. Chem. Phys.* **89**, 6753 (1988).
- ³³J. H. D. Eland, R. Frey, A. Kuestler, H. Schulte, and B. Brehm, *Int. J. Mass Spectrom. Ion Phys.* **22**, 155 (1976).
- ³⁴M. Krauss, J. A. Walker, and V. H. Dibeler, *J. Res. Natl. Bur. Stand. Sect. A* **72**, 281 (1968).
- ³⁵M. Tsuji, K. Matsumura, T. Funatsu, Y. Nishimura, and H. Obase, *J. Chem. Phys.* (to be published).
- ³⁶A. Cornu and R. Massot, *Compilation of Mass Spectral Data* (Heiden, London, 1966).
- ³⁷M. T. Jones, T. D. Dreiling, D. W. Setser, and R. N. McDonald, *J. Phys. Chem.* **89**, 4501 (1985).
- ³⁸W. Kischlat and H. Morgner, *J. Electron Spectrosc. Relat. Phenom.* **35**, 273 (1985).